JOURNAL OF GEOPHYSICAL RESEARCH, VOL. 105, NO. A6, PAGES 12,955–12,974, JUNE 1, 2000

Phase transition-like behavior of the magnetosphere during substorms

M. I. Sitnov,[1,2] A. S. Sharma,[1] K. Papadopoulos,[1] D. Vassiliadis,[3]
J. A. Valdivia,[3,4] A. J. Klimas,[5] and D. N. Baker[6]

Abstract. The behavior of substorms as sudden transitions of the magnetosphere is studied using the *Bargatze et al.* [1985] data set of the solar wind induced electric field vB_s and the auroral electrojet index AL. The data set is divided into three subsets representing different levels of activity, and they are studied using the singular spectrum analysis. The points representing the evolution of the magnetosphere in the subspace of the eigenvectors corresponding to the three largest eigenvalues can be approximated by two-dimensional manifolds with a relative deviation of 10-20%. For the first two subsets corresponding to small and medium activity levels the manifolds have a pleated structure typical of the cusp catastrophe. The dynamics of the magnetosphere near these pleated structures resembles the hysteresis phenomenon typical of first-order phase transitions. The reconstructed manifold is similar to the "temperature-pressure-density" diagrams of equilibrium phase transitions. The singular spectra of vB_s, AL, and combined data have the power law dependence typical of second-order phase transitions and self-organized criticality. The magnetosphere thus exhibits the signatures of both self-organization and self-organized criticality. It is concluded that the magnetospheric substorm is neither a pure catastrophe of the low-dimensional system nor a random set of avalanches of different scales described by the simple sandpile models. The substorms behave like nonequilibrium phase transitions, with features of both first- and second-order phase transitions.

1. Introduction

Earth's magnetosphere is an open system and geomagnetic activity, consisting of storms and substorms, is its main response to the influence of the solar wind. The global coherence in the magnetospheric dynamics indicates that the magnetosphere is a dynamical system with low effective dimension [*Sharma*, 1995; *Klimas et al.*, 1996]. However, obtaining its effective dimension is not straightforward for a number of reasons. The techniques of phase space reconstruction and dimension estimation are developed for autonomous systems in general [e.g., *Abarbanel et al.*, 1993]. Although the application of these techniques to the auroral electrojet indices shows evidence that the magnetosphere is low-dimensional [*Vassiliadis et al.*, 1990; *Sharma*, 1995], the results are not conclusive. The extension of these techniques to input-output systems [*Casdagli*, 1992] is more appropriate for modeling the solar wind-magnetosphere system. The nonlinear filters relating the input (solar wind variables) to the output (AL index) show that a relatively small number of magnetospheric state variables dominate the dynamics [*Vassiliadis et al.*, 1995]. Moreover, the relatively small amount of geomagnetic and solar wind data required to make the best prediction indicates the nonlinearity of solar wind-magnetosphere coupling [*Vassiliadis et al.*, 1996].

It appears that the geomagnetic activity is neither a simple linear response to the changes of the solar wind conditions nor an output of the autonomous system. Rather, there are elements of self-organization [*Haken*, 1975] in the geospace. The self-organization concept can be further elaborated along two main directions. The first one is the creation of specific nonlinear models of geomagnetic activity based on physical processes.

[1]Department of Astronomy, University of Maryland, College Park.
[2]On leave from Skobeltsyn Institute of Nuclear Physics, Moscow State University, Moscow, Russia.
[3]Universities Space Research Association, NASA Goddard Space Flight Center, Greenbelt, Maryland.
[4]Now at Departamento de Fisica, Facultad de Ciencias, Universidad de Chile.
[5]Laboratory for Extraterrestrial Physics, NASA Goddard Space Flight Center, Greenbelt, Maryland.
[6]Laboratory for Atmospheric and Space Physics, University of Colorado, Boulder.

Paper number 1999JA000279.
0148-0227/00/1999JA000279$09.00

One of the earliest examples of such an approach was the interpretation of the substorm as a thermal catastrophe [*Smith et al.*, 1986; *Goertz and Smith*, 1989]. The second direction is the reconstruction of the system dynamics directly from the data [*Sharma*, 1995]. Such approaches, namely, nonlinear filters [*Vassiliadis et al.*, 1995] and neural networks [*Gleisner and Lundstedt*, 1997; *Weigel et al.*, 1999], have very good prediction ability and are potential tools for space weather forecasting. However, these approaches do not yield directly the physical processes involved. This has led to models such as the dripping faucet and Faraday loop analogue models [*Baker et al.*, 1990; *Klimas et al.*, 1992], data-derived analogues based on transforming local-linear prediction models into dynamical systems of equations [*Klimas et al.*, 1997], and the low-dimensional magnetosphere-ionosphere coupling model [*Horton and Doxas*, 1996; *Horton et al.*, 1998] including its further development in terms of the inverse bifurcation sequence [*Horton et al.*, 1999]. In this work we explore further the reconstruction of dynamics from time series data to study the nature of sudden transitions in the magnetosphere during substorms.

The self-organization often implies metastability of the system, namely, a collection of temporarily stable states, with some of them being related to the others by relatively quick transition processes such as bifurcations or catastrophes [*Haken*, 1975]. This is similar to the the loading-unloading scenario in the Earth's magnetosphere during substorms. The metastability naturally implies the existence of low-dimensional manifolds, which the system is embedded in during the stable periods. Such a manifold may, however, have a complicated pleated structure as the relationship between input and output variables may be not one-to-one [*Casdagli*, 1992]. Recent analysis of magnetospheric data using autoregressive moving-average (ARMA) filters [*Vassiliadis et al.*, 1995] has given evidence in favor of such a pleated structure of the dynamical manifold through its better prediction ability with the use of the previous output data. The successful long-term prediction based on ARMA filters suggests that phenomena like dynamical chaos may not dominate the response of the magnetosphere to the solar wind input. Consequently, the expected dynamical manifold may have no fractal features and reproduce the abrupt substorm changes as well as seemingly random nature of the substrom onset according to the classical scenario of critical points of smooth functions [*Arnol'd*, 1975]. This scenario based on the catastrophe theory [*Gilmore*, 1993] is used in our study as a working hypothesis.

2. Magnetospheric Substorm As a Catastrophe

The theory of catastrophes describes abrupt changes in a system under slow changes of a control parameter. Mathematically, it is described by a class of differential equations, the so-called gradient systems [*Guckenheimer and Holmes*, 1983],

$$\frac{d\mathbf{z}}{dt} = -\frac{\partial U(\mathbf{z}, \mathbf{C})}{\partial \mathbf{z}}. \tag{1}$$

Catastrophes in such systems manifest as abrupt changes in the state variable $\mathbf{z}$ under slow variations of the effective potential U because of changes in the control parameters $\mathbf{C}$. For quasi-static states defined by

$$\frac{\partial U(\mathbf{z}, \mathbf{C})}{\partial \mathbf{z}} = 0 \tag{2}$$

the catastrophe is usually connected with the change in the number of local minima of the effective potential U. The concept of catastrophes is closely related to bifurcations, with the catastrophes considered as inverse bifurcations [*Haken*, 1975].

The nature of the catastrophe is determined by the number of control parameters and state variables involved. In particular, the simplest fold or A_2 catastrophe is represented by a transformation of the potential

$$U(z, c_1) = z^3 + 3c_1 z \tag{3}$$

from the function with the local minima $z_{1,2} = \sqrt{-c_1}$ ($c_1 < 0$) to a monotonous one ($c_1 > 0$) with the formation of the inflection point at $c_1 = 0$. This is illustrated in Figure 1, where the transition from linear to nonlinear instability at the catastrophe is due to the change in the form of the effective potential. It is often useful to distinguish between this genuine catastrophe and the dynamical regime when the system is able

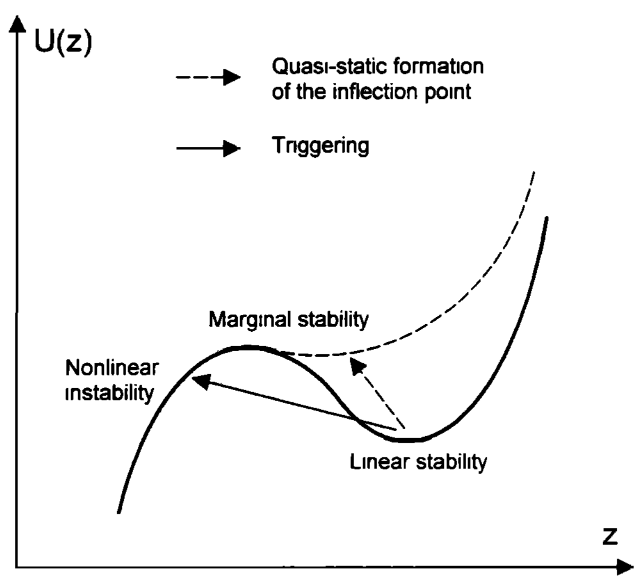

Figure 1. The effective potential evolution during the fold catastrophe (from solid to dashed line) and the corresponding dynamical regimes: delay convention regime, when the marginal stability should be reached (dashed arrow), and Maxwell convention regime, when the catastrophe starts because of the external trigger or noise (solid arrow).

to jump over the potential barrier before the inflection point is formed because of a small but finite amplitude of an external trigger or internal fluctuations (Figure 1). The corresponding limiting cases are known in catastrophe theory as Delay and Maxwell conventions [*Gilmore*, 1993]. In the substorm phenomenology they may be identified with spontaneous substorm onsets [*Dmitrieva and Sergeev*, 1983; *Henderson et al.*, 1996] and those triggered by the solar wind [*Caan et al.*, 1975; *Sergeev et al.*, 1996a], respectively.

The model of substorms as a fold catastrophe was proposed by *Smith et al.* [1986] and *Goertz and Smith* [1989] on the basis of the resonant absorption of Alfven waves in the plasma sheet boundary layer. On similar lines a model of explosive ballooning instability has been recently proposed for substorms, solar flares and tokamak disruptions by *Cowley and Artun* [1997] and *Hurricane et al.* [1998] on the basis of the detonation concept. In connection with the most natural process of the energy release during substorms, namely, the spontaneous reconnection in the tail current sheet, the first catastrophe model was in fact formulated by *Galeev and Zelenyi* [1976]. According to their model the energy of the appropriate eigenmode (tearing mode) may be positive because of the stabilizing influence of trapped electrons, which corresponds to the positive curvature of the effective potential in Figure 1 near the local minimum. As a result, the tearing mode becomes stable in the presence of any dissipation. On the other hand, there are gaps in the parameter space of the system where the sign of the energy of the tearing mode changes. This corresponds to the change of the sign of the curvature of the potential energy curve in Figure 1 after the formation of the inflection point and results in the loss of stability under finite dissipation. This interesting model of a metastable tail current sheet has not received the attention it deserves mainly because of its more rigorous results [*Lembege and Pellat*, 1982; *Pellat et al.*, 1991], which leave no room for the instability gaps. Recently, however, *Sitnov et al.* [1998; 1999] have shown that the sufficient stability condition of the tearing mode is not as restrictive as was suggested by *Lembege and Pellat* [1982] and the marginal stability may be reached through the shielding effect of transient electrons under the small electron-to-ion temperature ratio.

The fold catastrophe alone cannot explain the whole sequence of substorm dynamics because the potential (3) does not include the recovery of the system after the catastrophe. *Goertz and Smith* [1989] recognized that the system should evolve back toward its initial state along different phase diagrams than those describing the original (direct) catastrophe. The recovery phase can be described by introducing a second control parameter in the scheme of substorms as a cusp or A_3 catastrophe as proposed by *Lewis* [1991]. The main features of this scenario are represented by the potential

$$U(z, c_1, c_2) = z^4 + 2c_1 z^2 + 4c_2 z, \qquad (4)$$

with two control parameters c_1 and c_2. The state parameter in this model is the nightside magnetic field orientation, while the control parameters are $c_1 = -$(open) flux + const and $c_2 =$ (nightside − dayside) (reconnection rate). The potential (4) may have either one minimum corresponding to one equilibrium state of the system or two minima corresponding to different equilibrium states. The onset of the substorm is represented as a disappearance of the upper minimum due to a local fold catastrophe. The condition (2) for the potential (4) looks like a folded surface in the three-dimensional space

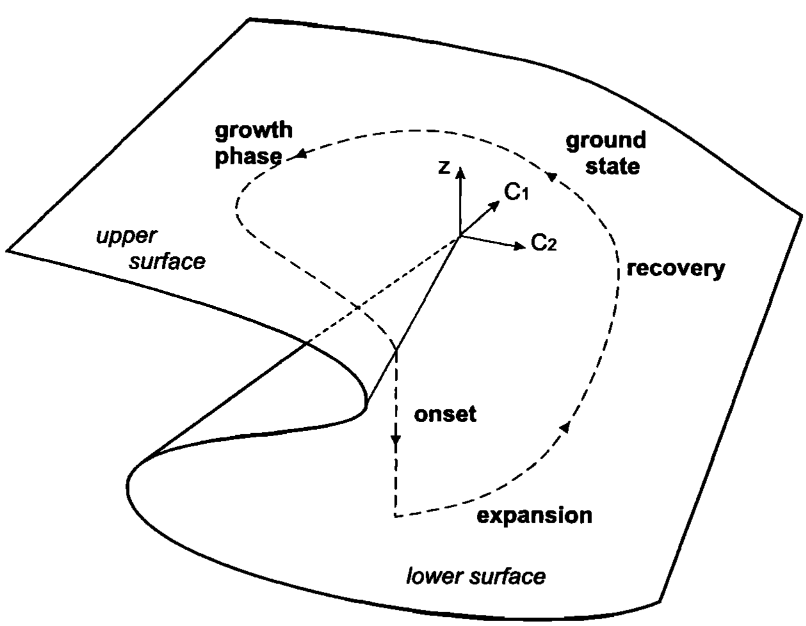

Figure 2. The cusp catastrophe manifold (2) for substorms as interpreted by *Lewis* [1991]. The evolution of an isolated substorm is shown by dashed arrows.

(c_1, c_2, z) Figure 2, and all the dynamical states available to the magnetosphere are supposed to lie on this surface. Figure 2 also shows a typical substorm cycle including growth, onset, and recovery phases as suggested by *Lewis* [1991]. Since the transition to catastrophe depends on more than one variable, it becomes possible to explain the variability in the energy release during individual substorms and, in particular, the difference between pseudobreakups and conventional substorms.

The catastrophe model for substorms will, however, remain only an interesting qualitative hypothesis unless either the specific physical processes responsible for the catastrophic behavior are revealed or the manifold that has the fold structure is derived from the observational data. In this paper we address the second issue by using the techniques of phase space reconstruction from observational data. This effort is aimed at developing a framework for a global description of substorm dynamics.

3. Singular Spectrum Analysis of the $vB_s - AL$ Data

We use the database of *Bargatze et al.* [1985] (hereafter referred to as BBMH) containing 34 intervals of correlated measurements of the auroral electrojet index AL, the solar wind bulk speed v, and the southward component of the magnetic field B_s ($B_s = -B_z$ for $B_z < 0$ and $B_s = 0$ for $B_z > 0$, where the interplanetary magnetic field is expressed in GSM coordinates), each 1-2 days in length. The database is separated into three subsets (1-15, 16-26, and 27-34), each containing approximately the same number of points ($\sim 13,000$) and representing different levels of activity. BBMH have shown the qualitaively different behavior of the magnetosphere associated with directly driven and loading-unloading parts of the response for low, medium, and high activity levels estimated on the basis of the median values of the AL index. While some of the subsequent studies on bimodal filters [*Blanchard and McPherron*, 1993] did not reveal a consistent dependence on the level of activity in the magnetosphere, other studies [*Smith and Horton*, 1998] have also found such a dependence. This difference in the results is explained by *Smith and Horton* [1998] as due to the difference of the data sets used in the above studies and, in particular, the use of isolated substorm data in the study of *Blanchard and McPherron* [1993]. The inference about the dependence of the magnetospheric response upon the activity level has been substantiated very recently by *Weigel et al.* [1999]. They have shown in particular that the use of the gated neural network, where the BBMH data set is explicitly divided into three intervals (1-10, 11-20, 21-32), results in a much better performance of the network, as compared to its original version [*Hernandes et al.*, 1993], especially for strong substorms.

To reconstruct the manifold on which the trajectory of substorm dynamics lies, we use a modification of the singular spectrum analysis (SSA) [*Broomhead and King*, 1986] to include both input and output time series. The input is the product vB_s. This variable is a measure of the solar wind induced electric field and the reconnection rate near the Earth's magnetopause. The output variable is the auroral electrojet index AL. The trajectory matrix describing the dynamics of the solar wind-magnetosphere system can be constructed from AL and vB_s as

$$\mathbf{Y}=\begin{bmatrix} AL(t_1)..\,AL(t_1-(m-1)\tau) & -vB_s(t_1)..-vB_s(t_1-(m-1)\tau) \\ AL(t_2)..\,AL(t_2-(m-1)\tau) & -vB_s(t_2)..-vB_s(t_2-(m-1)\tau) \\ .\ \ ..\ \ \ \ . & .\ \ ..\ \ \ \ . \\ .\ \ ..\ \ \ \ . & .\ \ ..\ \ \ \ . \\ AL(t_N)..\,AL(t_N-(m-1)\tau) & -vB_s(t_N)..-vB_s(t_N-(m-1)\tau) \end{bmatrix} \tag{5}$$

where the typical value of the dimension m of the embedding space is 32 and that of the time delay τ is 2.5 min. The matrix $\mathbf{Y}$, constructed using the time delay embedding technique [*Abarbanel et al.*, 1993; *Sharma*, 1995], contains information about variables other than the original ones and can provide a complete description of the system. To make input and output parameters more homogeneous, they are normalized separately by the corresponding standard deviations. The matrix $\mathbf{Y}$ can be represented in the form

$$\mathbf{Y} = \mathbf{UWV}^T \tag{6}$$

using singular value decomposition (SVD) [*Press et al.*, 1992]. Here $\mathbf{U}$ is an $N \times 2m$ matrix; $\mathbf{W}$ is a $2m \times 2m$ diagonal matrix; and $\mathbf{V}$ is a $2m \times 2m$ orthogonal matrix. $\mathbf{W}$ contains the SSA eigenvalues, while $\mathbf{V}$ and $\mathbf{U}$ determine the SSA eigenvectors and the projections of the original trajectory matrix along those eigenvectors $P_i \equiv U_i w_i = (\mathbf{YV})_i$, respectively.

In the ideal case this decomposition would reveal the number of linearly independent vectors that can be constructed from the trajectory in the embedding space [*Broomhead and King*, 1986]. For real noisy systems it allows for (1) estimation of the effective number of variables describing the essential dynamical behavior of the system by selecting diagonal elements w_i considerably above the others, which form the noise floor, (2) determination of the corresponding directions in $2m$ dimensional space and projection of the data along them, thus making it possible to effectively reduce the noise and observe the corresponding attractor (if it exists) in the embedding space. The formal problem of finding dynamical correlations in the data array $\mathbf{Y}$ is equivalent to the eigenvalue problem for the $N \times N$ structure matrix $\mathbf{YY}^T$, which in turn is reduced to the problem of finding $2m$ eigenvectors w_i^2 of the $2m \times 2m$ covariance matrix $\mathbf{Y}^T\mathbf{Y}$. SSA may be considered as a modification of Fourier or wavelet analyses because of its data-derived basic functions [*Preisendorfer*, 1988; *Danilov and Solntsev*, 1997].

In the analysis of the output data alone, namely, the AL index [*Sharma*, 1993; *Sharma et al.*, 1993], the study of the correlation integral based on this technique yields an estimate of the effective (embedding) dimension of the magnetosphere as an autonomous system. However, the magnetosphere is a driven system and representing it as an autonomous system has limitations. This may explain the variance of these results with those of nonlinear filters [*Vassiliadis et al.*, 1995]. It is expected that the use of both input and output time series in SSA will help not only in estimating the effective number of degrees of freedom of the magnetosphere but also in revealing the essential input-output relationships.

3. 1. Singular Spectrum, Effective Dimension, and Original Eigenvectors

The singular spectra of the three subsets of BBMH data are computed for time delays $\tau = 2.5, 5.0$, and 7.5 min and for embedding dimension $m = 16$, 32, and 48. The total delay values ($= m\tau$ in these cases) are in the range 40-120 min and in most cases cover the whole loading-unloading timescale range for substorms (20-60 min). The eigenvalues for the case $m = 32$ and $\tau = 2.5, 5.0$, and 7.5 min are shown in Figure 3a. Figure 3b shows the eigenvalues for $\tau = 2.5$ and $m = 16$, 32, and 48. These spectra show no clear noise floor for small values m, but this should not be interpreted as an indication of a large effective dimension of the system because SSA itself is a linear technique and cannot be directly used for dimension assessment [*Gibson et al.*, 1992]. Figure 3 still shows that the two or three leading eigenvalues actually dominate over the others. This shows that the study of the system in the reduced phase space created by the leading eigenvectors would allow us to reduce effectively the noise and reveal the essential dynamical features of the system.

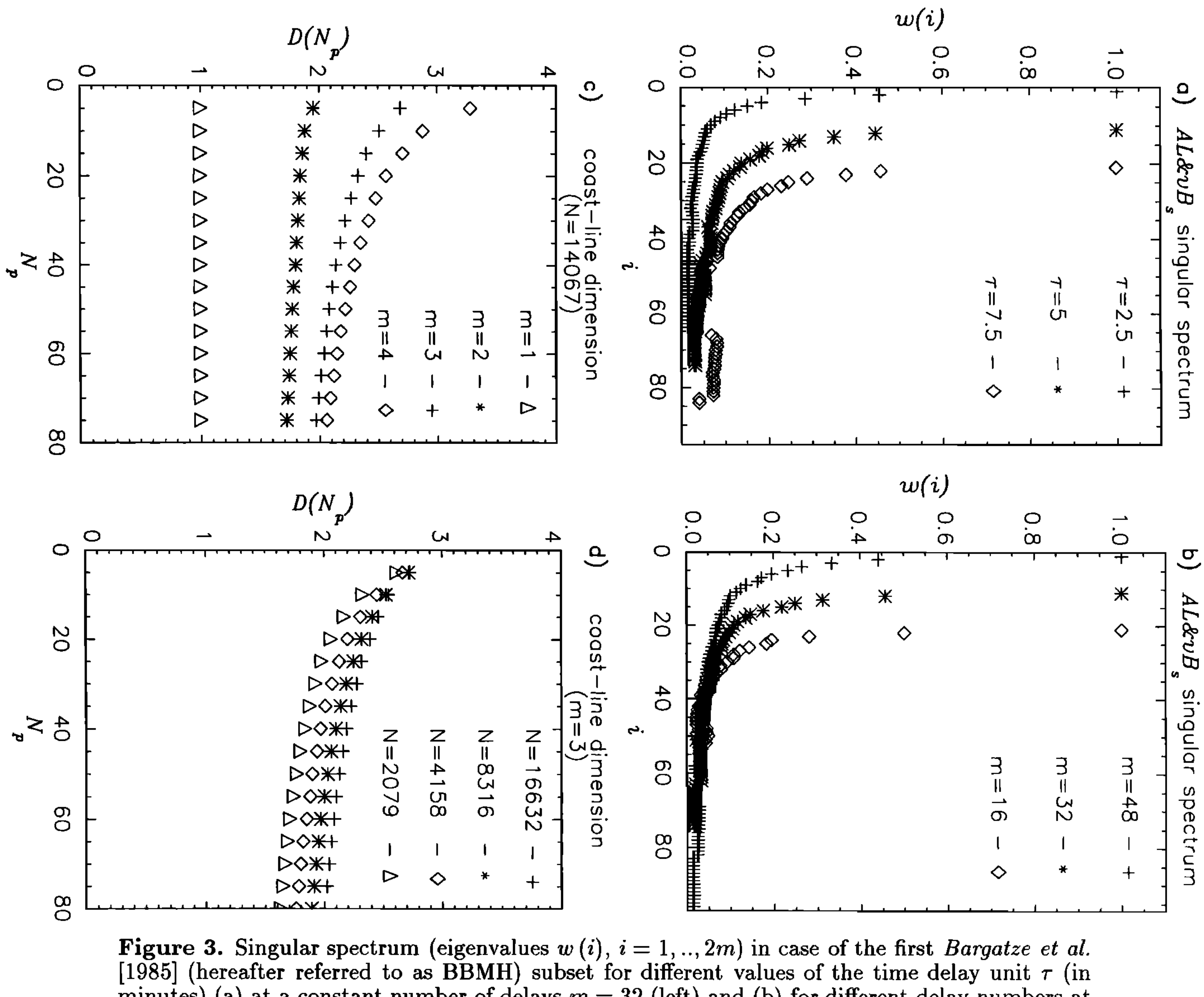

Figure 3. Singular spectrum (eigenvalues $w(i)$, $i = 1,..,2m$) in case of the first *Bargatze et al.* [1985] (hereafter referred to as BBMH) subset for different values of the time delay unit τ (in minutes) (a) at a constant number of delays $m = 32$ (left) and (b) for different delay numbers at constant $\tau = 2.5$ min. The results of assessing the fractal dimension of the first BBMH subset as a function $D(N_p)$ of box partition N_p along each of m directions in $m-$dimensional embedding space for (c) different embedding dimensions $m = 1 - 4$ and (d) different numbers N of the trajectory points.

This suggestion is confirmed by the results of a direct assessment of the fractal dimension of the system trajectory. The coast-line dimension of the trajectory set in the embedding space [*Abarbanel et al.*, 1993] is given by

$$D_f \approx D(N_p) = \log(N_t) / \log(N_p), \quad (7)$$

where N_p is the number of partitions of the three-dimensional cube embedding the trajectory along each principal component P_i and N_t is the number of cubes created because of this partitioning and containing at least one point of the trajectory. Figure 3c shows typical signatures of the finite dimension; namely, it shows that the dimension is close to the embedding dimension till $m = 3$ and then it remains close to $D_f = 2$ in spite of further increase of m. This implies that the trajectory lies on a two-dimensonal manifold (surface) embedded into a three-dimensional subspace. The effect of increasing the total number of points used to verify the dimension estimate in the case of $m = 3$ is shown in Figure 3d. Figure 3d shows that the above estimate of the dimension is sustained only for the largest scales ($N_p \leq N_* \sim 20$). The issue of increasing the total number of points necessary to obtain a reliable effective (correlation) dimension has been noted earlier [*Roberts*, 1991] in the computation of the correlation dimension of the AL index without taking into account spurious autocorrelation effects. Using the SSA and taking into account the autocorrelation effect yield an upper bound of this dimension $D \leq D_c \sim 2.5$ with the embedding dimension $m \sim 4-5$ [*Sharma et al.*, 1993]. While the actual dimension associated with substorm is still a subject of debate [*Sharma*, 1995; *Klimas et al.*, 1996], the above assessment using the coast-line method seems to be quite sufficient for the reconstruction of magnetospheric dynamics. The reconstruction is achieved by projecting the original trajectory matrix onto the subspace created by the main SSA eigenvectors and approximating that projection by a smooth manifold (line, surface, etc.). Taking into account the above results, we limit ourselves to three main eigenvectors (corresponding to $m = 3$) and approximate the data set in this three-dimensional space by a two-dimensional suface (corresponding to $D_f = 2$).

The original eigenvectors corresponding to the three largest eigenvalues are shown in Figure 4, where shading corresponds to the output (AL) and black to the input (vB_s). On the basis of Figure 4 the first and second eigenvectors may be interpreted as directly driven and loading-unloading components of the activity, respectively, with the loading scale $\Delta t \sim 1$ hour ($\sim 30\tau$) being found the same regardless of τ and m. Similar conclusions concerning the first two eigenvectors were reached recently by *Sun et al.* [1998] in their study of the map of the equivalent current system on the basis of the International Magnetospheric Study (IMS) database [*Kamide et al.*, 1982]. They used a modification of the SSA technique and identified the map projections given by the first and second SSA eigenvectors with the well-known idealized current systems DP2 and DP1, respectively.

3. 2. Rotated Eigenvectors

The principal SSA components shown in Figure 4 represent the leading features of substorm dynamics. Each eigenvector is composed of the output and input components and thus there are six variables, making it difficult to visualize the manifold. Most surface plotting routines need also some basic plane (x, y) to plot the surface as the single-valued function $z = F(x, y)$. Such simple plotting might give us completely improper results in the case of a folded surface. For instance, the plane (c_1, z) is suitable as a basic plane for plotting the surface drawn in Figure 2, while the original plane (c_1, c_2) is not. To resolve this problem as well as to facilitate further interpretation of the results we rotate the eigenvectors as

$$\begin{Bmatrix} \mathbf{V}_1 \to \mathbf{V}_1\cos\alpha + \mathbf{V}_2\sin\alpha \\ \mathbf{V}_2 \to -\mathbf{V}_1\sin\alpha + \mathbf{V}_2\cos\alpha \end{Bmatrix} \otimes \begin{Bmatrix} \mathbf{V}_2 \to \mathbf{V}_2\cos\beta + \mathbf{V}_3\sin\beta \\ \mathbf{V}_3 \to -\mathbf{V}_2\sin\beta + \mathbf{V}_3\cos\beta \end{Bmatrix} \quad (8)$$

and then perform the inversions in three-dimensional space of the original eigenvectors shown in Figure 4. The goal of each rotation is to minimize or maximize the ratio between the output ($j = 1-32$) and input ($j = 33-64$) parts of each eigenvector so that the resultant variables approach either the control or state parameter of some catastrophe model. Taking into account the close resemblance between the SSA and the conventional Fourier transforms, we used different measures of the eigenvector parts for the first and second rotations. When adjusting the first rotation, we tried to minimize/maximize the appropriate averaged components $|\sum_{j=1}^{32} V_i(j) / \sum_{k=33}^{64} V_i(k)|$, while during the second rotation, the first harmonic $|\sum_{j=1}^{32} (j-16.5) V_i(j) / \sum_{k=33}^{64} (k-48.5) V_i(k)|$ was selected for the same purpose. The adjustments are achieved through trial and error and led to the following transformations. For the first BBMH subset, $\alpha = 0.785$ and $\beta = 0.25$; for the second BBMH subset, $\alpha = 0.785$ and $\beta = -0.20$ with an inversion of the new vector $\mathbf{V}_3$; and for the third BBMH subset $\alpha = -0.785$ with a rotation of $\mathbf{V}_3$ and the new vector $\mathbf{V}_2$, and $\beta = 0.25$. The resulting basis vectors are shown in Figure 5 (we shall use the term "basis vectors" instead of "eigenvectors" because the above transformations can destroy the diagonal form of the original matrix $\mathbf{W}$ in (6) in the three-dimensional subspace of the main eigenvectors). From the variables in Figure 5 it is clear that the output (AL) contribution is dominant in the second vector (Figures 5b, 5e, and 5h), while the other two (Figures 5a, 5d, and 5g and Figures 5c, 5f, and 5i) are related mainly to the input component.

The principal components $P_i = (\mathbf{YV})_i$ conjugated to the main basis vectors $\mathbf{V}_i$ turn out to be surprisingly close to the control and state parameters in the scheme

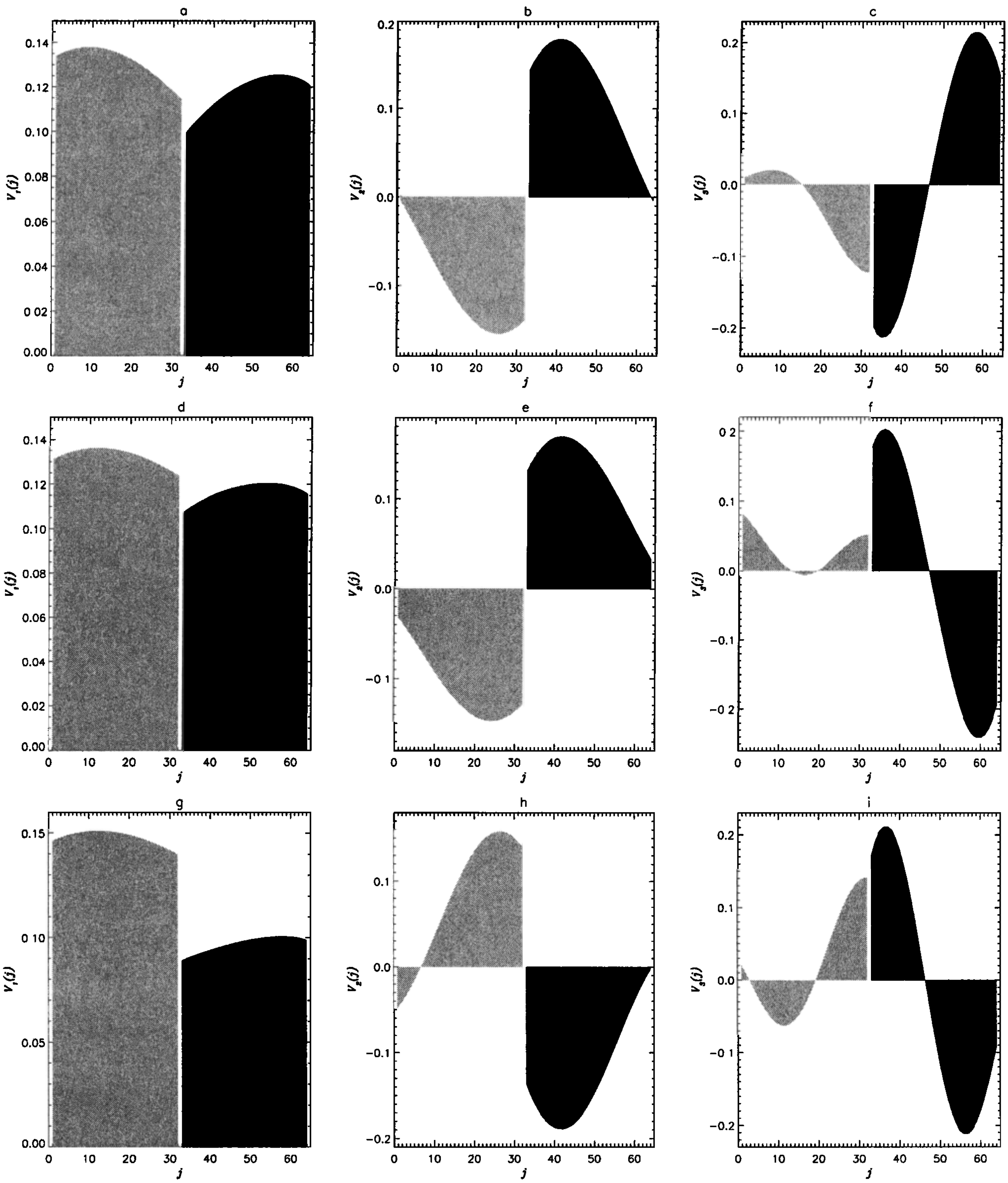

Figure 4. Triplets of eigenvectors $V_i(j)$, $i = 1, 2, 3$, and $j = 1, .., 2m$ corresponding to the three largest eigenvalues for the (a)-(c) first, (d)-(f) second, and (g)-(i) third BBMH subsets with $\tau = 2.5$ min and $m = 32$. The AL and vB_s parts of the eigenvectors corresponding to the structure of the trajectory matrix (5) are shown by shading and black filling, respectively.

of the substorm as a catastrophe [*Lewis*, 1991]. In particular, the first principal component P_1 corresponding to the basis vector $\mathbf{V}_1$ (Figures 5a, 5d, and 5g) is formed by integrating the parameter $-vB_s$ in time over the period of about an hour, a typical loading timescale associated with the energy input in the magnetosphere due to the dayside reconnection during the growth phase. Therefore, taking into account the conventional inter-

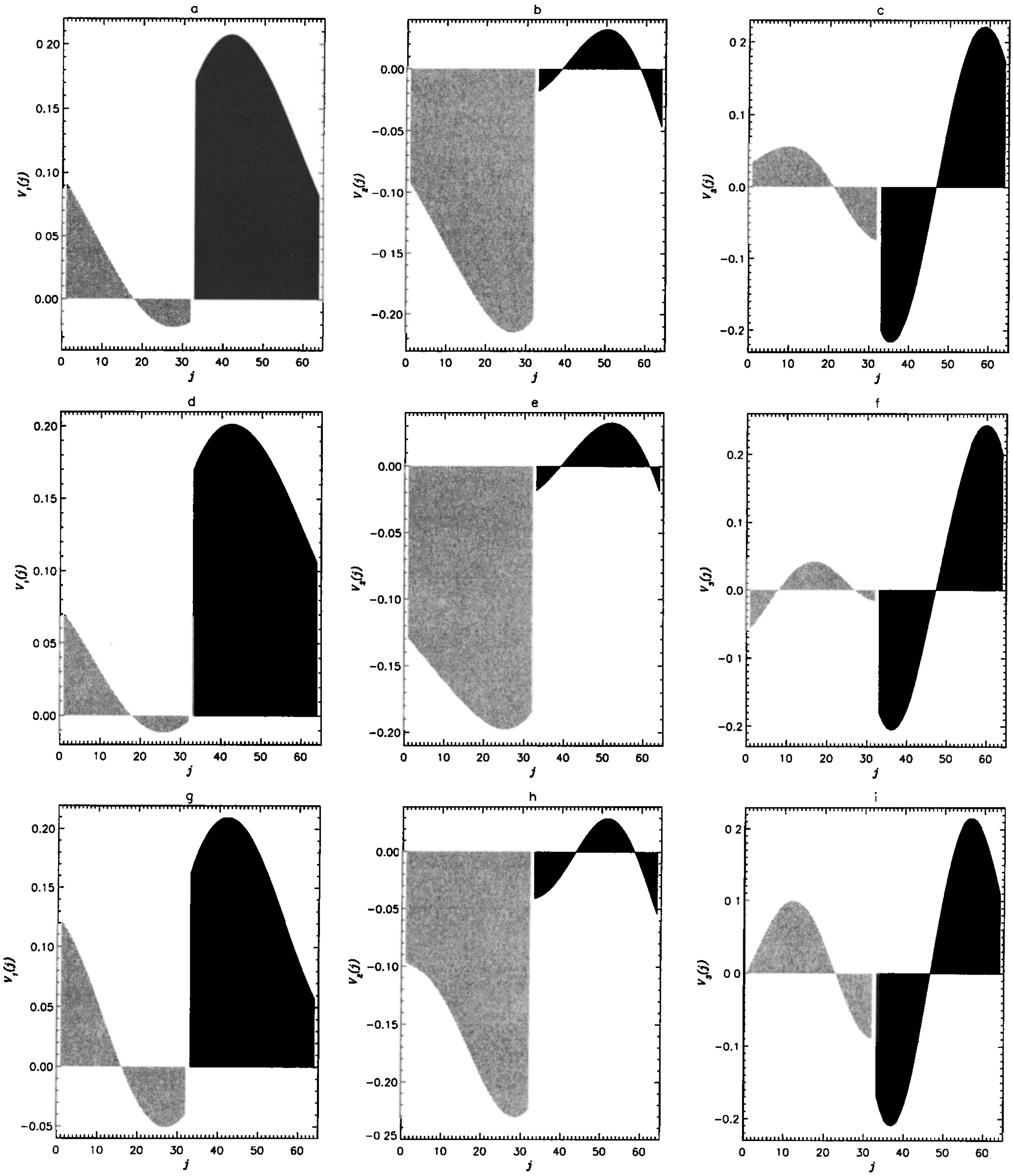

Figure 5. The three main eigenvectors from Figure 4 after rotation and inversion.

pretation of the parameter vB_s as a measure of the inductive (reconnection) electric field near the dayside magnetopause, P_1 is analogous to the control parameter $c_1 = -(\text{open})\ \text{flux} + \text{const}$. The relatively limited (~ 1 hour) period of integration necessary to produce this principal component from vB_s implies that the reconnection rate due to the dayside merging should be large enough to overcome the plasma sheet convection, which returns the magnetic flux back to the magnetosphere, and this limits from above the possible duration of the growth phase. The third principal component P_3 corresponding to the basis vector $\mathbf{V}_3$ (Figure 5c, 5f, and 5i) reflects the difference between the nearly immediate (with the time delay $<\sim 20$ min) value of vB_s and

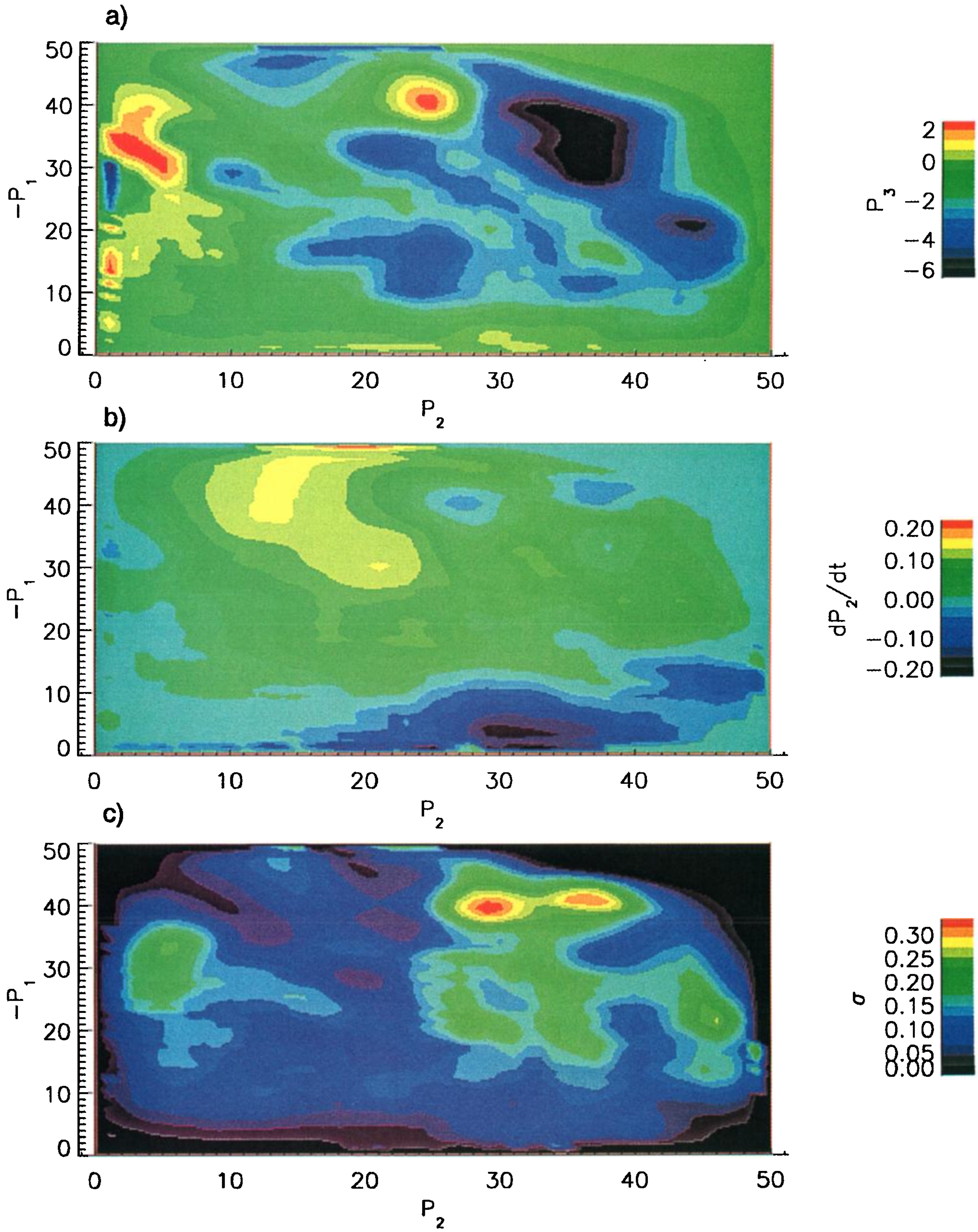

Plate 1. (a) Color-coded image of the approximating surface drawn in Figure 6d, (b) the rate of variation of the parameter P_2, and (c) the relative deviation (9) of the original data points from the approximating surface in Figure 6d as functions of the principal components P_2 and $-P_1$.

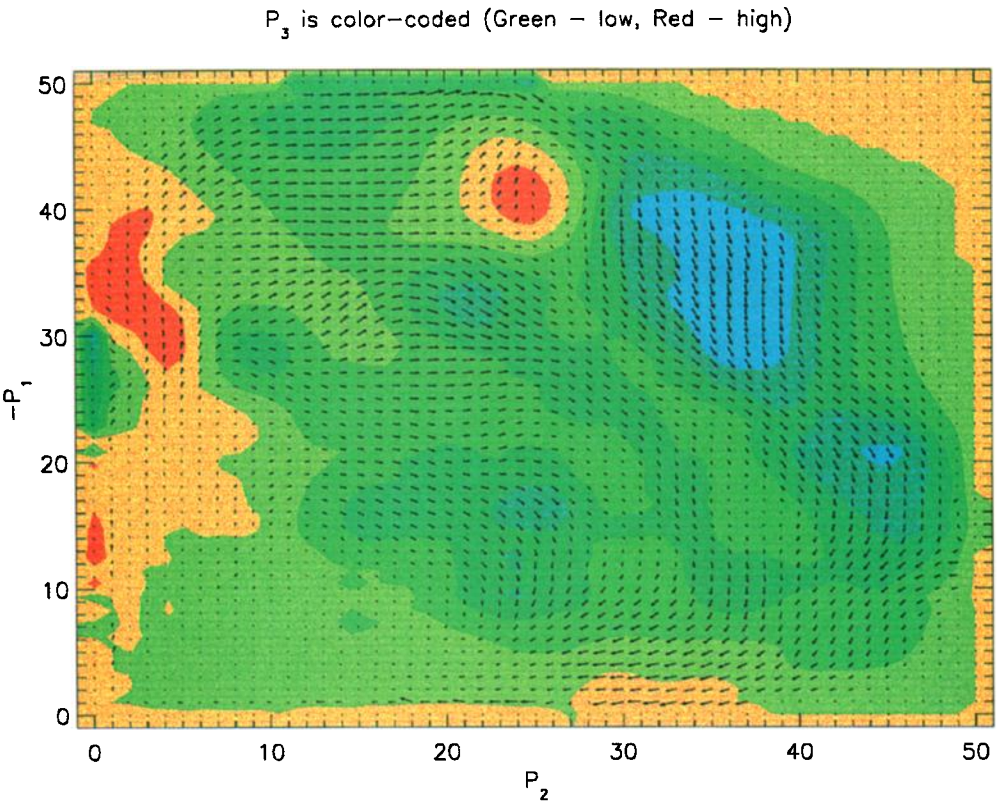

Plate 2. Analogue of Plate 1a with the overplotted velocity field of the parameters P_2 and $-P_1$.

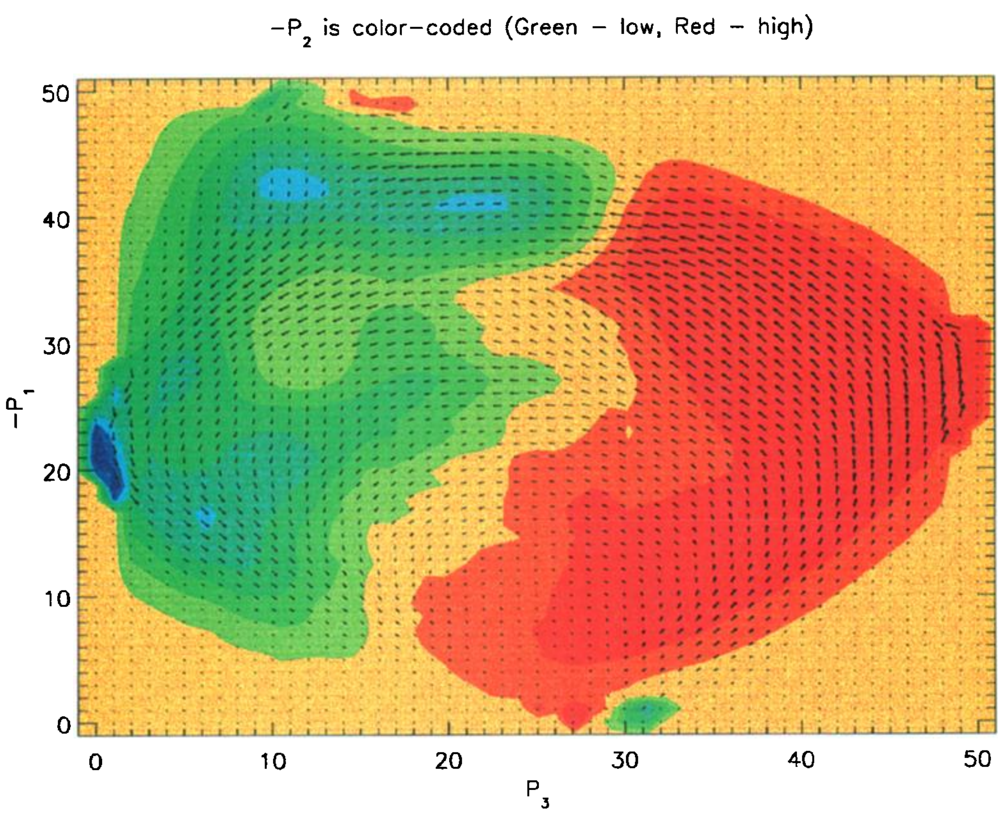

Plate 3. Color-coded approximating surface and the appropriate velocity field for the first BBMH subset with excluded hysteretic intervals on the plane $(P_3, -P_1)$ and the corresponding velocity field. The component P_3 is shifted as $P_3 \to P_3 + 25$.

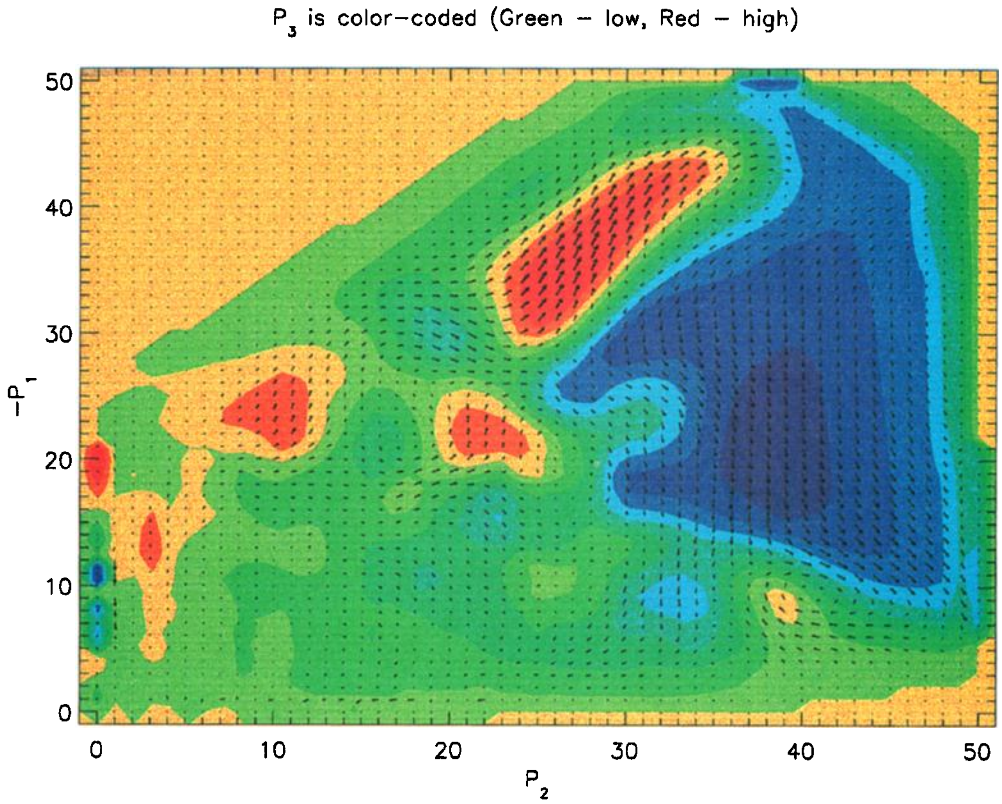

Plate 4. Analogue of Plate 2 for the second BBMH subset.

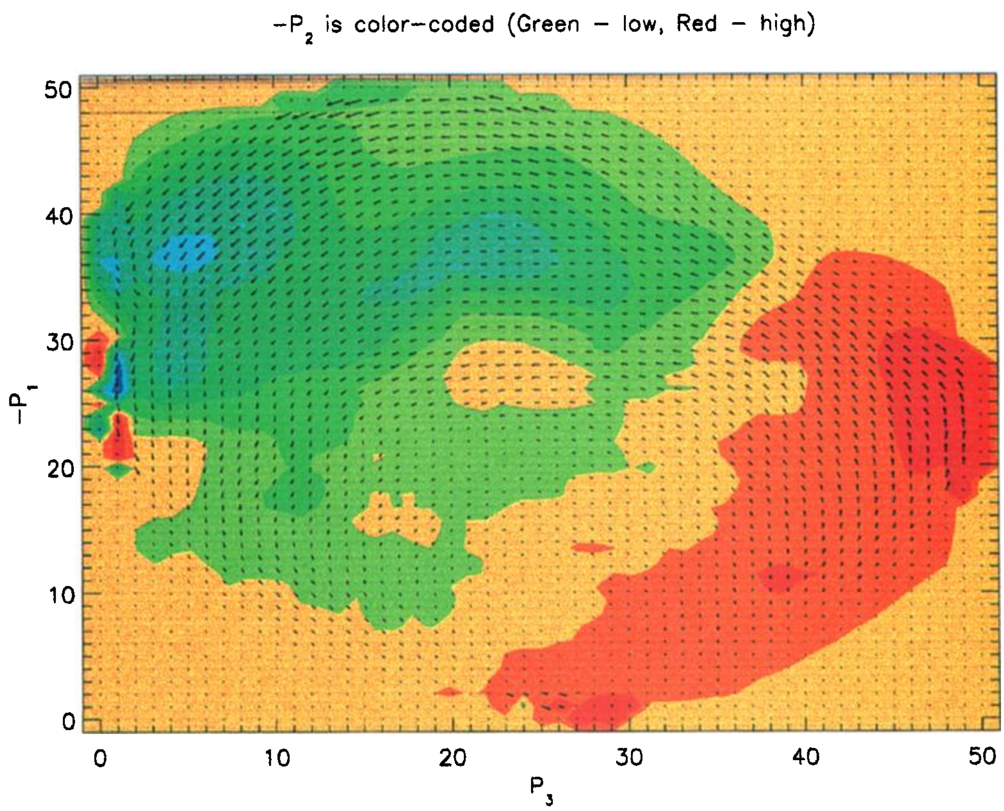

Plate 5. Analogue of Plate 3 for the second BBMH subset.

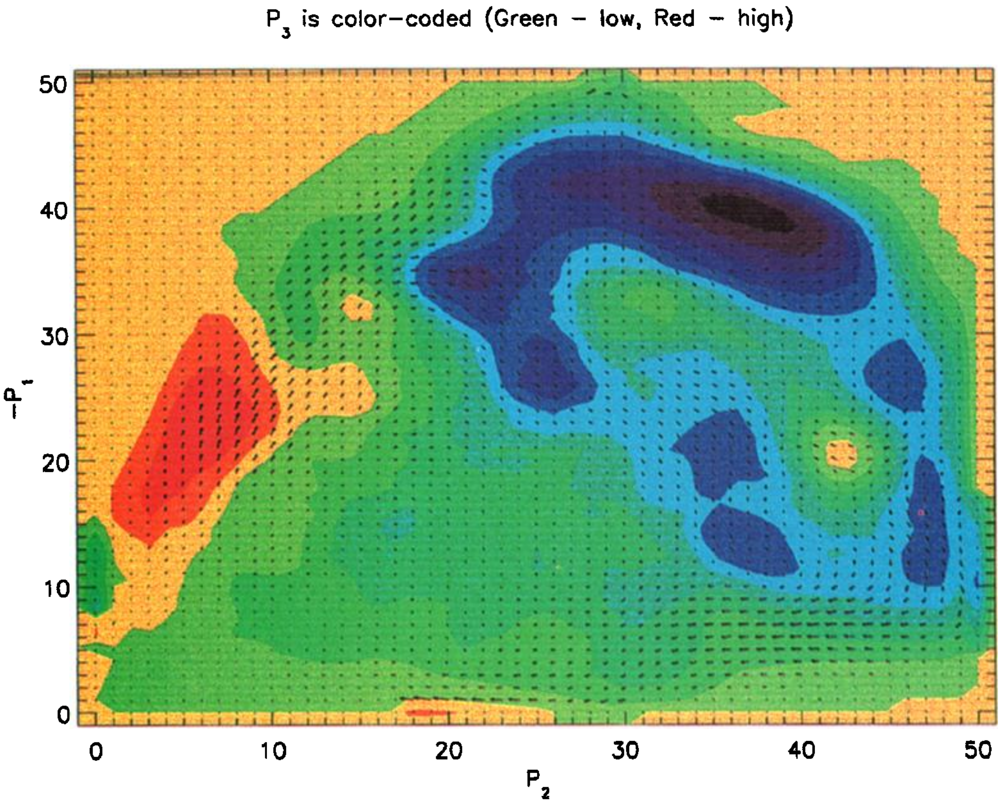

Plate 6. Analogue of Plate 2 for the third BBMH subset.

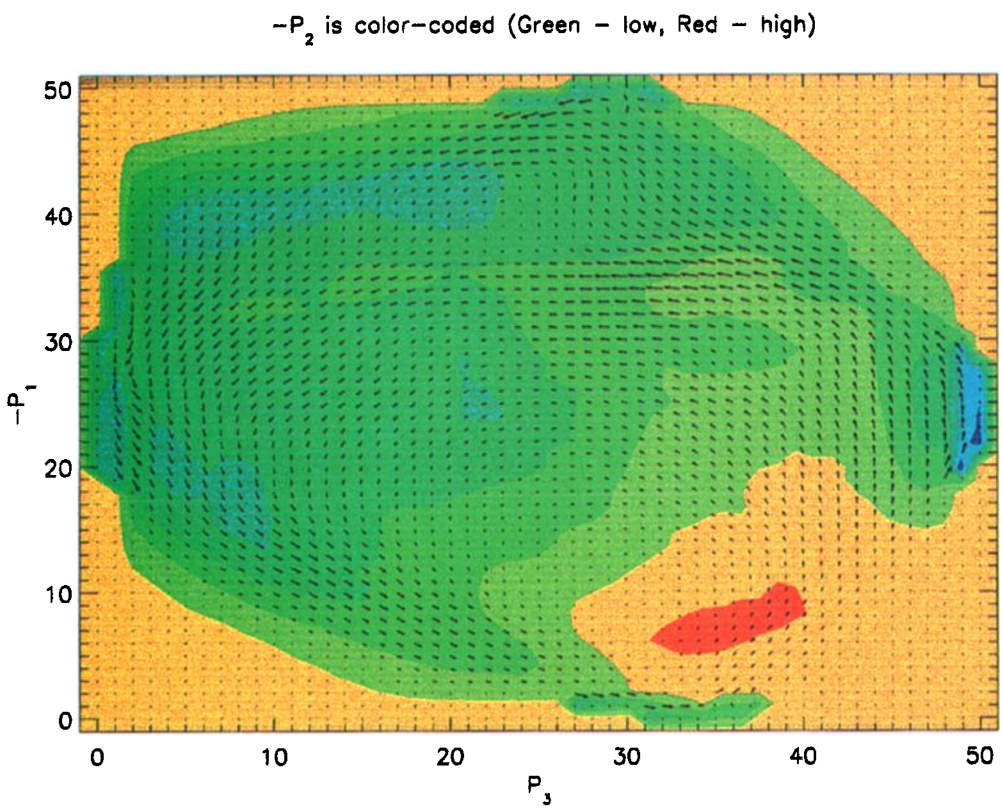

Plate 7. Analogue of Plate 3 for the third BBMH subset.

its earlier values (time delay around one hour). The second principal component P_2 produced by the basis vector $\mathbf{V}_2$ (Figures 5b, 5e, and 5h) apparently represents mainly the time-integrated AL index (with the inversion of sign).

In fact, neither control parameter in the *Lewis* [1991] scheme can be directly connected with the SSA parameters because neither the nightside reconnection rate nor the plasma sheet convection rate are explicitly involved in the analysis. These control parameters can be effectively represented, nevertheless, by the appropriate SSA principal components. In particular, the parameter P_3 can mimic the control parameter because of the time delay between the first (negative) bay in Figures 5c, 5f, and 5i and the second (positive) one, which is comparable with the time of signal propagation from the magnetopause to the distant tail. As a result, the first bay reflects the dayside reconnection rate (nearly immediate values of vB_s), while the second bay takes effectively into account the contribution of the nightside reconnection because of its opposite sign and the appropriate delay (past values of vB_s affect the nightside reconnection). In the parameter P_1 the nightside reconnection is also implicitly taken into account by decreasing the envelope of its output part. Finally, in spite of the fact that the state parameter z in the scheme of *Lewis* [1991] (nightside magnetic field orientation) is rather uncertain and while the auroral zone geomagnetic index AL is not the best measure of the substorm activity, both z (if measured in the near-Earth tail) and P_2 (integrated $-AL$) characterize the state of the magnetosphere during substorms.

4. Phase Transition-Like Behavior During Substorms

4. 1. Principal Components for the First BBMH Subset

For the first BBMH subset the evolution of the magnetosphere as a dynamical system in the subspace of three main eigenvectors as well as its approximation by the smooth two-dimensional manifold (taking into account the rotations and inversions described in the previous subsection) are reflected in Figure 6 and Plates 1-3. Figures 6a-6c represent, in particular, the two-dimensional projections of the magnetosphere's trajectory to planes $P_1 - P_3$ of the principal components, corresponding to the rotated and inverted eigenvectors $\mathbf{V}_1 - \mathbf{V}_3$ from Figure 5. The analysis of the projections yields the following picture of the substorm cycle in terms of these principal components. The growth phase of the substorm corresponds to the growth of the absolute value of the parameter P_1 (accumulation of the magnetic flux) from the nearly zero level at constant and close to zero parameter P_2 (no activity reflected by AL). The ex-

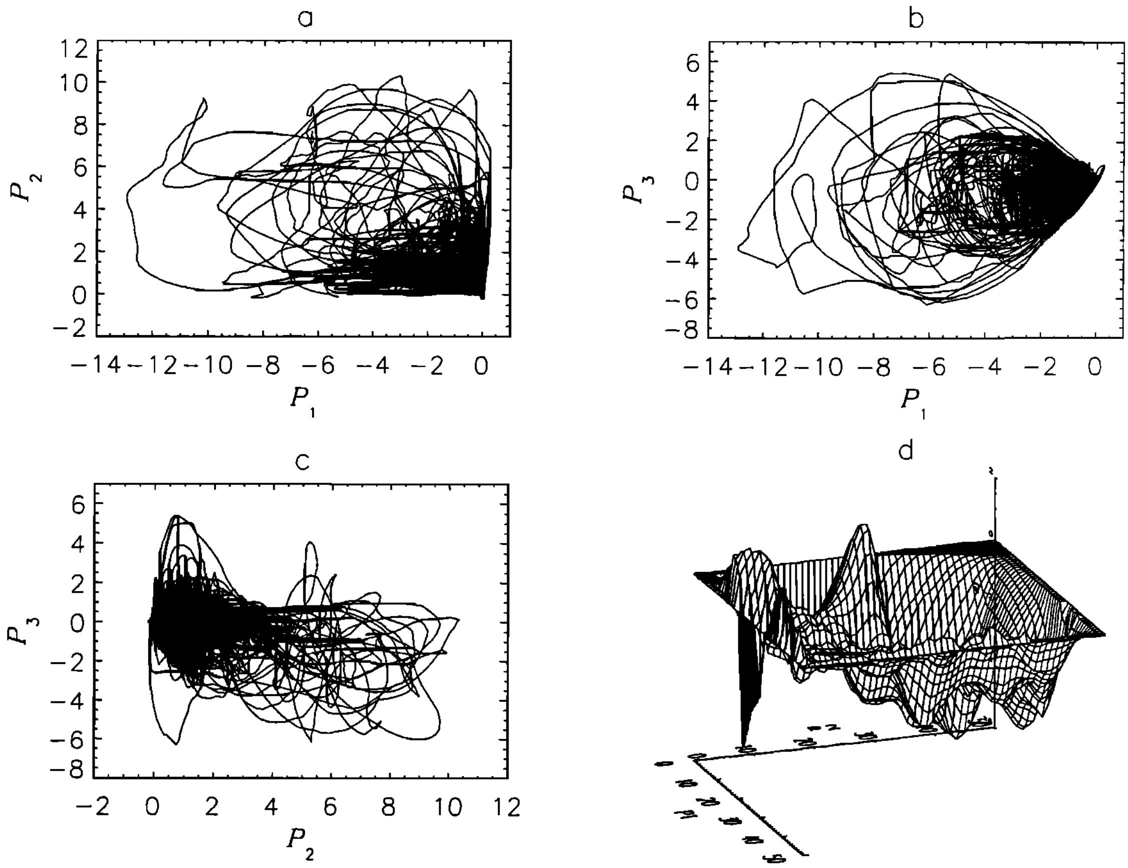

Figure 6. (a)-(c) One-dimensional and (d) two-dimensional approximations of the first BBMH subset in three-dimensional space.

plosive phase corresponds to the growth of P_2 (start of activity in the form of AL decrease) associated usually with the decrease of the component P_3 down to negative values (northward turning of the interplanetary magnetic field) under approximately constant P_1 (saturated magnetic flux). This effect is well known as a possible prerequisite of substorms [*Caan et al.*, 1975; *Rostoker*, 1983] either because of the reduction in the magnetospheric convection [*Lyons*, 1995] or the additional intensification of the tail current [*Alexeev and Bobrovnikov*, 1997]. Moreover, it can be directly observed in some of the BBMH database analyzed here, namely, intervals 1, 2, 7, 9, and 12-17. The recovery phase (which can hardly be separated from the subsequent growth phase) corresponds to the restoration (growth) of the parameters P_1, $-P_2$ and P_3 to zero levels.

The surface shown in Figure 6d is obtained by a triangulation of the tarjectory set on the plane (P_1, P_2). This procedure allows one to resolve the problem of the irregular distribution of the points on this plane. For each point $i \in (P_1, P_2)$ of the regular grid there is only one triangle $\left(P_{1(i)}^{(j)}, P_{2(i)}^{(j)}\right)$, where $j = 1, 2, 3$, created by projections of the original data points in which the point i is embedded. Then the third coordinate of the point i may be determined using the linear interpolation (by a plane surface) of the triangle $\left(P_{1(i)}^{(j)}, P_{2(i)}^{(j)}, P_{3(i)}^{(j)}\right)$ in three-dimensional space. The important distinctive feature of the surface in Figure 6d is the valley in its left part, which is analogous to the upper part of the fold structure in Figure 2. It is apparently formed because in some substorm cycles, the dayside reconnection rate turns out to be large again at the end of the expansion phase, although this new portion of the incoming magnetic flux cannot substantially affect the activity ($P_2 \simeq$ const) because of the different (low) global energy state of the magnetosphere after the onset. A representative of such dynamical behavior of the magnetosphere may be the convection bay [*Pytte et al.*, 1978; *Sergeev et al.*, 1996b] following a typical substorm (V. A. Sergeev, private communication, 1999). In the physics of nonequilibrium first-order phase transitions this phenomenon is well known as hysteresis [*Brokate and Sprekels*, 1996], and the valley left from the central peak in Figure 6d corresponds to the state of a superheated liquid in the case of liquid-gas transition [*Landau and Lifshitz*, 1974].

Plate 1a represents the color contour plot analogue of the surface plot of Figure 6d, and the valley mentioned above corresponds to the green-blue region to the left of the central red spot. If this valley region actually describes the local fold catastrophe within the cusp catastrophe picture suggested by *Lewis* [1991], it should be also the region of the fastest (catastrophic) changes of the state parameter of the system, represented in our case by the parameter P_2 (integrated AL index). This is confirmed by Plate 1b, where the parameter dP_2/dt is color-coded on the same plane $(P_2, -P_1)$ as in Plate 1a.

The results of estimating the errors due to the approximation of the original set of points in three-dimensional space by the smooth surface shown in Figure 6d and Plate 1a are shown in Plate 1c. The deviation σ of each original data point i from the smooth surface is estimated as

$$\sigma = \frac{\sqrt{\left[P_{3(i)} - (1/4)\sum_{k=1}^{4} \widetilde{P}_{3(i)}^{(k)}\right]^2}}{P_{3\max} - P_{3\min}}, \qquad (9)$$

where $\widetilde{P}_{3(i)}^{(k)}$ is the Taylor expansion of the smooth approximation $P^{(s)}(P_1, P_2)$ in Figure 6d at $(P_{1(i)}, P_{2(i)})$ relative to each of the four points $\left({P_1}^{(k)}, {P_2}^{(k)}\right)$ forming the regular grid cell that contains the point $(P_{1(i)}, P_{2(i)})$:

$$\begin{aligned}\widetilde{P}_{3(i)}^{(k)} &= P^{(s)}\left({P_1}^{(k)}, {P_2}^{(k)}\right) \\ &+ \left(P_{1(i)} - {P_1}^{(k)}\right) \frac{\partial P^{(s)}}{\partial P_1}_{|{P_1}^{(k)}, {P_2}^{(k)}} \\ &+ \left(P_{2(i)} - {P_2}^{(k)}\right) \frac{\partial P^{(s)}}{\partial P_2}_{|{P_1}^{(k)}, {P_2}^{(k)}} . \qquad (10)\end{aligned}$$

$P_{3\max}$ and $P_{3\min}$ are the maximum and minimum values of the principal component P_3 over the whole trajectory set, respectively. According to Plate 1c the relative error in the valley region is not the largest one, and it does not exceed 10%. The relative deviation of the actual data from the approximately two-dimensional surface is rather small ($\sim 10-20\%$) nearly everywhere in the plane $(P_2, -P_1)$. The only exceptions seen on the right of the pleat feature are produced largely because of the very steep profile of the pleat (see, e. g., Figure 6d) where the expansion (10) is hardly valid.

The averaged evolution of the magnetosphere on or near the reconstructed surface is shown in Plates 2 and 3. In particular, Plate 2 is an analogue of Plate 1a with the vector field of "velocities" constructed from dP_2/dt and $-dP_1/dt$ shown by the arrows. The prototype of this data-derived flow picture is the typical substorm cycle suggested by *Lewis* [1991] and is drawn by dashed arrows in Figure 2. It is clearly seen from Plate 2 that the trajectories entering the pleated region (red spot in the center) reveal the hysteresis phenomenon during which at the same input parameters, P_1 and P_3, the system can be in different states P_2 depending on its history. This phenomenon, while being very interesting in itself, strongly complicates the plotting of the approximate manifold on the plane (P_1, P_3). Fortunately, the specific substorm activations responsible for this phenomenon are rather sparse (otherwise, there would be a ridge instead of the single peak in Figure 6d and Plates 1a and 2), and the corresponding activity intervals in the original data may be accurately detected and deliberately excluded from the data set (since the begin-

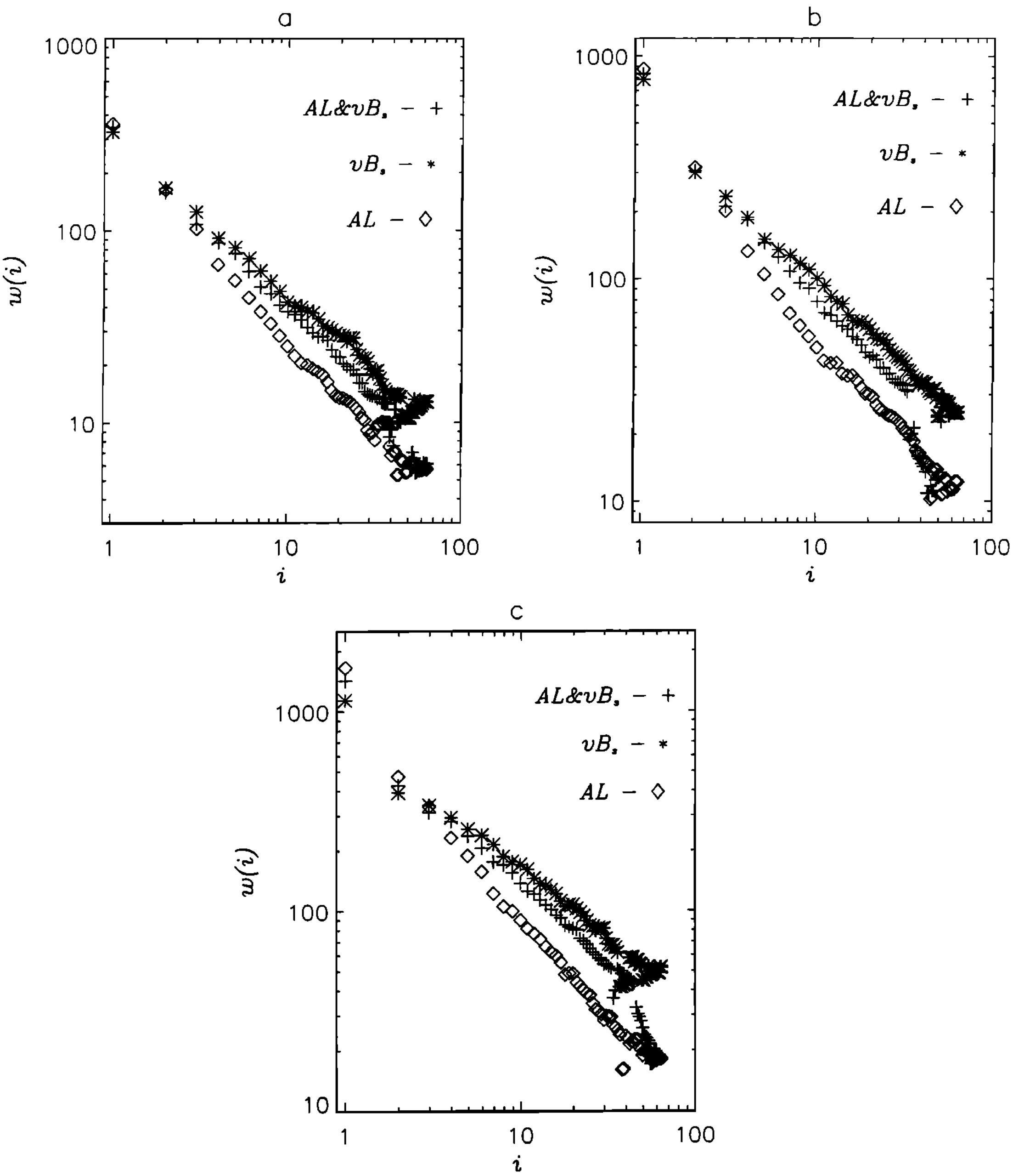

Figure 7. Log-Log plots of SSA eigenvalues for AL and vB_s parameters alone as well as for the combined data in cases of the (a) first, (b) second, and (c) third BBMH subsets; $\tau = 2.5$ min, $m = 32$ in case of combined data, and $m = 64$ for input and output parameters alone.

ning and the end of each such interval corresponds to zero or small activity as well as solar wind input, this operation does not change the whole structure of the BBMH data set). As a result, we obtain the pleated manifold shown in Plate 3. This manifold as well as the averaged dynamical picture of the actual substorm activity, with the velocity field $(dP_3/dt, -dP_1/dt)$ superimposed, are again very similar to the original picture suggested by *Lewis* [1991] and shown in Figure 2. In particular, the counterclockwise circulation of the flow in Plate 3 corresponds to the similar circulation of the substorm prototype from Figure 2 when projected on the plane $(-c_2, -c_1)$. The manifold resembles also the "temperature-pressure-density" diagrams well known in the physics of conventional equilibrium phase transitions [*Stanley*, 1971]. The transition associated with the substorm onset takes place between the regions of relatively high (close to zero) and low (more negative) values of the parameter $-P_2$ coded by red and green-blue colors, respectively. These regions correspond to high and low levels of the effective potential energy of the magnetosphere and, inversely, to low and high levels of its dynamical activity (analogue of the kinetic energy) reflected by the local value of the parameter $-AL$. The yellow nearly vertical band separating green-blue and red regions (the remainder of the yellow region, which surrounds the red and green-blue domains, contains no data) corresponds to the first-order phase transition curve, and it is the upper part of this bridge-like feature that reflects a typical substorm onset phenomenon. The suddenness of the activity changes in Plate 3 may be assessed by the speed of the color change along the arrow multiplied by the length of the arrow itself. One can see, in particular, that this parameter is much larger near the upper edge of the yellow bridge-like band corresponding to the well-developed onsets as compared to the same parameter taken at its lower edge and corresponding to the small activations close to the ground state of the magnetosphere (Figure 2).

If we develop further the analogy with phase transitions, then the region at the lower center part of Plate 3 (close to the lower edge of the yellow band mentioned above) should correspond to the critical point with the scale invariant behavior. Such a behavior is actually revealed in the substorm activity data in the form of various power law spectra [*Tsurutani*, 1990; *Takalo et al.*, 1993; *Lui*, 1998] and can be interpreted in terms of self-organized criticality, a dynamical analogue of the second-order phase transitions [*Chapman et al.*, 1998; *Consolini*, 1998; *Lui*, 1998]. Moreover, as it is shown in Figure 7a, the singular spectra of AL and vB_s and the combined data also demonstrate similar power law dependence (SSA in this case is very close to conventional Fourier expansions). The case of $AL - vB_s$ combined is, in fact, the analogue of the left sequence of points from Figure 3a made in log-log format. We discuss these analogies in more detail in sections 4.2 and 5.2.

4. 2. Second and Third BBMH Subsets

The analogues of Plates 2 and 3 and Figure 7a for the second and third BBMH subsets are presented in Plates 4-7 and Figures 7b and 7c. In particular, Plate 4 shows that the valley region associated with the local fold catastrophe and the whole cusp structure is well defined and even more impressive in the case of medium activity than in the case of low activity. On the contrary, Plate 6, corresponding to the case of high activity reveals no considerable hysteresis signatures. At the same time a comparison of Plates 3, 5, and 7 reveals a rather gradual disappearance of the pleated structure of the two-dimensional manifold in the form of the temperature-pressure-density diagram (with excluded hysteresis loops) with increasing activity level. The almost complete diappearance of the pleat signatures in the case of the third BBMH subset may be naturally explained by the Maxwell dynamical regime of the magnetosphere's transition to a low energy state when the system (magnetosphere) may overcome the potential barrier before the formation of the inflection point and, as a result, the pleated landscape of the cusp catastrophe manifold may disappear because of the reduction of the upper part of the fold in Figure 2.

It should be emphasized that apart from the disappearance of some signatures of the first-order phase transitions for the second and third BBMH subsets the whole dynamical picture including other phase transition aspects remains qualitatively the same notwithstanding the increase of the activity level. This is seen from a comparison of the appropriate SSA eigenvalues (Figure 7), eigenvectors (Figures 4 and 5), and clockwise (Plates 2, 4, and 6) and counterclockwise (Plates 3, 5, and 7) circulation flows and concerns, first of all, the scale invariant behavior shown in Figure 7, which is the primary distinctive feature of second-order phase transition and self-organized criticality.

5. Discussion and Conclusion

The technique of phase space reconstruction from the observational data, in particular, singular spectrum analysis, has been used to analyze the substorm data set of BBMH. The analysis has led to the following conclusions.

1. The low effective dimension of the magnetosphere as a dynamical system on the largest substorm scales was confirmed and its dynamic trajectory lies on a two-dimensional surface in the three-dimensional space of the main SSA eigenvectors.

2. The main eigenvectors corresponding to the three largest SSA eigenvalues used to obtain the appropriate basis vectors by rotation and inversion can be interpreted in terms of of the specific control and state parameters of the cusp catastrophe model of the substorm activity [*Lewis*, 1991].

3. The two-dimensional surface approximating the trajectories of the magnetosphere in the corresponding three-dimensional embedding space resembles the pleated surface typical of a cusp catastrophe. The complementary circulation flows (velocity fields) also agree with the cusp catastrophe model.

4. Hysteresis phenomena typical for the catastrophe evolution and the first order phase transitions are shown for the first and second subsets of the BBMH data set.

5. There is a close resemblance between the two-dimensional surface with excluded hysteresis intervals and the temperature-pressure-density diagrams of the conventional equilibrium phase transitions.

6. The singular spectrum of the input (vB_s), output (AL), and combined data obeys the power laws typical for the second-order phase transitions near the critical point and the self-organized criticality.

5. 1. Is the Substorm a Catastrophe?

The features of substorms, listed above, support the scenario suggested by *Lewis* [1991] on the basis of the theory of catastrophes. At the same time the deviations from the ideal catastrophe model are also essential and meaningful. It is worth noting here that the catastrophes and the critical behavior may be considered as different aspects of the same physical phenomenon, namely, phase transitions [*Landau*, 1937; *Devonshire*, 1954; *Thom*, 1972; *O'Shea*, 1977; *Haken*, 1983; *Gilmore*, 1993; *Jensen*, 1998]. The absence of convincing evidences of low effective dimension on smaller scales as well as the power law form of the entire SSA spectrum suggests that the structure of the manifold in the vicinity of the cusp point is more complicated than is described by the theory of catastrophes and, in particular, by the *Lewis* [1991] model. On the other hand, the simplest catastrophe scenario with the quasi-static loading of the system turns out to be considerably modified by the increase of activity due to either a high level of internal fluctuations in the magnetosphere or the triggered nature of many substorms [*Caan et al.*, 1975]. The systematic influence of these effects resulting in the disappearance of the pleated structure of the manifold due to the "underbarrier" transitions shown in Figure 1 can be inferred, in particular, from comparison of Plates 2, 4, and 6 and Plates 3, 5, and 7. These effects and those near the cusp point are detected above the SSA noise floor and cannot therefore be ignored in future models of the substorm activity.

One of the main physical inferences of our analysis is that there should exist a global instability responsible for isolated substorm onsets, which looks like the genuine fold catastrophe under the Delay convention dynamical regime and which is reflected by the pleated structure of the substorm dynamics manifold in the case of small and medium activity cases. Such a global substorm instability has been suggested by *Baker et al.* [1998] on the basis of observational and theoretical considerations. This is a nonclassical nonlinear instability [*Sitnov et al.*, 1997; *Chang*, 1998; *Sitnov and Sharma*, 1998, *Hurricane et al.*, 1998] in the sense that the corresponding plasma physical model can be neither that of the linear instability nor that of the finite amplitude instability and the marginal linear stability should be reached prior to substorm. In the case of finite amplitude instability the fold structures in the Maxwell convention dynamical regime are expected to be fuzzy, more typical of the high activity case.

5. 2. Is the Magnetosphere a Sandpile or a Dripping Faucet?

During the past decade a new interesting concept of the self-organized criticality (SOC) based on the simple model of a sandpile [*Bak et al.*, 1987] has been used widely in the interpretation of catastropic processes in open spatially extended systems. Briefly, a system is in a state of SOC when the statistics of the energy release events (avalanches) reveal no characteristic length or timescale and, as a result, the appropriate spectra obey power laws. Contrary to conventional second-order phase transitions near the critical point, which also exhibit scale invariant behavior [*Willson*, 1983], SOC was shown to be robust and to arise spontaneously without the tuning of system parameters. The SOC concept has been used for the explanation of substorm activity [*Chang*, 1992, 1998; *Lui*, 1998; *Consolini*, 1997; *Chapman et al.*, 1998] on the basis of the observation that some spectra obey power laws [*Tsurutani et al.*, 1990; *Takalo et al.*, 1993; *Ohtani et al.*, 1995, 1998; *Lui*, 1998]. The phenomenological picture of this multiscale aspect of the substorm activity has been described in detail in the review of *Sergeev et al.* [1996a].

It turns out, however, that the dynamics of open and spatially extended systems including sandpiles themselves contain features that are not described by the conventional SOC models. For instance, real sandpiles may behave in a manner more reminiscent of a first-order transition (similar to the ordinary fold catastrophe) than a second order one [*Nagel*, 1992]. In the case of substorms, explicit violations of the SOC behavior are present in the form of the statistics of chorus events seen at the ground and particle injections in the near-Earth magnetosphere [*Borovsky et al.*, 1993; *Pritchard et al.*, 1996; *Smith et al.*, 1996]. In particular, the intensity and occurence rate of substorms have a probability distribution with a well-defined mean. These results are consistent with the earlier and more recent results on the assessment of the effective dimension of the magnetosphere [*Klimas et al.*, 1996] and the efficient prediction of the substorm activity on the basis of the local linear autoregressive filters [*Vassiliadis et al.*, 1995], which are summarized in the form of the concepts of the magnetosphere's self-organization (SO) [*Sharma*, 1995, *Klimas et al.*, 1996], global substorm instability [*Baker et al.*, 1998], and the simple analogues of the type of a dripping faucet [*Baker et al.*, 1990; *Klimas et al.*, 1992; *Horton and Doxas*, 1996, 1998; *Horton et al.*, 1998] in the place of a sandpile. Thus one has to conclude that real open and spatially extended systems demonstrate their double SOC-SO nature.

We also observe this double SOC-SO nature of the substorm phenomenon in the results of the SSA analysis of the BBMH data where a the power law singular spectrum coexists with indications of the low dimension of the system within some limited interval of scales and a relatively well defined cusp catastrophe manifold. Moreover, the analogy between the reconstructed manifold and the temperature-pressure-density diagrams of conventional phase transitions provides an interesting explanation of this nature. Specifically, we suggest that the substorm phenomenon is a set of the nonequilibrium phase transitions including both the second-order transitions (analogues of SOC) and the first-order ones (based on the SO concept), which are organized in the same manner as in the equilibrium case when the critical curve (as the locus of the first-order transitions) ends at the critical point where the second-order transition occurs. According to our analysis the substorm onsets resembling the first-order transitions are relatively large. Probably, they are associated with the global reconfiguration of the system including the formation of a near-Earth neutral line and a plasmoid. The phenomena on smaller scales are more reminiscent of the second-order transitions with no global reconfiguration. They reveal, instead, the power law distribution of the energy over scales typical of turbulent plasmas and other spatially extended systems modeled by the mathematical sandpiles. Thus the exhaustive description of avalanche-like events in open spatially extended systems like the Earth's magnetosphere requires more sophisticated dynamical models than the simplest mathematical analogues of the dripping faucet or the sandpile. There are already some advanced cellular automata models of substorms that explicitly take into account the SO aspect through varying coherence length in the effective one-dimensional sandpiles [*Chapman et al.*, 1998]. Also, both SO and SOC behaviors are revealed in the model of *Takalo et al.* [1999].

Acknowledgments. The authors wish to thank Victor Sergeev for informative comments and valuable discussions. The research at the University of Maryland was supported by NSF grants ATM-9626622 and ATM-9713479 and NASA grant NAG5-1011. M.I.S. acknowledges also the partial support from the Competitive Centre of Basic Research of the Russian Federation Education Department.

Janet G. Luhmann thanks Wendell C. Horton and Wei Sun for their assistance in evaluating this paper.

References

Abarbanel, H. D., R. Brown, J. J. Sidorovich, and T. S. Tsimring, The analysis of observed chaotic data in physical systems, *Rev. Mod. Phys.*, *65*, 1331, 1993.

Alexeev, I. I., and S. Y. Bobrovnikov, Dynamics of magnetospheric tail current sheet during substorm (in Russian), *Geomagn. Aeron.*, *37*, 24, 1997.

Arnol'd, V. I., Critical points of smooth functions and their normal forms, in *Russian Math. Surveys*, *30*, 1, 1975.

Bak, P., C. Tang, and K. Wiesenfeld, Self-organized criticality: An explanation of 1/f noise, *Phys. Rev. Lett.*, *50*, 381-384, 1987.

Baker, D. N., A. J. Klimas, R. L. McPherron, and J. Büchner, The evolution from weak to strong geomagnetic activity: An interpretation in terms of deterministic chaos, *Geophys. Res. Lett.*, *17*, 41, 1990.

Baker, D. N., T. I. Pulkkinen, J. Buchner, and A. J. Klimas, Substorms: A global magnetospheric instability, in *Substorms-4: International Conference on Substorms-4, Lake Hamana, Japan, March 9-13, 1998*, edited by S. Kokubun and Y. Kamide, p. 231, Terra Sci., Tokyo, 1998.

Bargatze, L. F., D. N. Baker, R. L. McPherron, and E. W. Hones Jr., Magnetospheric impulse response for many levels of geomagnetic activity, *J. Geophys. Res.*, *90*, 6387, 1985.

Blanchard, G. T., and R. L. McPherron, A bimodal representation of the response function relating the solar wind electric field to the *AL* index, *Adv. Space Res.*, *13*(4), 71, 1993.

Borovsky, J. E., R. J. Nemzek, and R. D. Belian, The occurence rate of magnetospheric-substorm onsets: Random and periodic substorms, *J. Geophys. Res.*, *98*, 3807, 1993.

Brokate, M., and J. Sprekels, *Hysteresis and Phase Transitions*, Springer-Verlag New York, 1996.

Broomhead, D. S., and G. P. King, Extracting qualitative dynamics from experimental data, *Physica D*, *20*, 217, 1986.

Caan, M. N., R. L. McPherron, and C. T. Russel, Substorm and interplanetary magnetic field effects on the magnetic tail lobes, *J. Geophys. Res.*, *80*, 191, 1975.

Casdagli, M., A dynamical system approach to modelling input-output systems, in *Nonlinear Modeling and Forecasting, SFI Stud. Sci. Complexity*, vol. XII, edited by M. Casdagli and S. Eubank, p. 265, Addison-Wesley-Longman, 1992.

Chang, T., Low dimensional behaviour and symmetry breaking of stochastic systems near criticality: can these effects be observed in space and in the laboratory?, *IEEE Trans. Plasma Sci.*, *20*, 691, 1992.

Chang, T., Multiscale intermittent turbulence in the magnetotail, in *Substorms-4: International Conference on Substorms-4, Lake Hamana, Japan, March 9-13, 1998*, edited by S. Kokubun and Y. Kamide, p. 431, Terra Sci., Tokyo, 1998.

Chapman, S. C., N. W. Watkins, R. O. Dendy, P. Helander, and G. Rowlands, A simple avalanche model as an analogue for magnetospheric activity, *Geophys. Res. Lett.*, *25*, 2397, 1998.

Consolini, G., Sandpile cellular automata and magnetospheric dynamics, in *Proceedings of the 8th GIFCO Conference, Cosmic Physics in the Year 2000: Scientific Perspectives and New Instrumentation*, 8-10 April 1997, edited by S. Aiello et al., Soc. Ital. di Fis., Bologna, Italy, 1997.

Cowley, S. C. and M. Artun, Explosive instabilities and detonation in magnetohydrodynamics, *Phys. Rep.*, *283*, 185, 1997.

Danilov, D. L., and V. N. Solntsev, Caterpillar techniques: The main ideas and implementation methods (in Russian), in *Principal Components of the Time Series*, p. 307, edited by D. L. Danilov and A. A. Zhigliavskii, St. Petersburg State Univ., St. Petersburg, Russia, 1997.

Devonshire, A. F., Theory of ferroelectrics, *Adv. Phys.*, *3*, 85, 1954.

Dmitrieva, N. P., and V. A. Sergeev, The spontaneous and induced onset of the explosive phase of a magnetospheric substorm and the duration of its preliminary phase, *Geomagn. Aeron. Engl. Transl.*, *23*, 380, 1983.

Galeev, A. A., and L. M. Zelenyi, Tearing instability in plasma configurations, *Sov. Phys. JETP, Engl. Transl.*, *43*, 1113, 1976.

Gibson, J. F., J. D. Farmer, M. Casdagli, and S. Eubank, An analytic approach to practical space reconstruction, *Physica D*, *57*, 1, 1992.

Gilmore, R., *Catastrophe Theory for Scientists and Engineers*, Dover, Mineola, New York, 1993.

Gleisner, H., and H. Lundstedt, Response of the auroral electrojets to the solar wind modeled with neural networks, *J. Geophys. Res.*, *102*, 14,269, 1997.

Goertz, C. K., and R. A. Smith, The thermal catastrophe model of substorms, *J. Geophys. Res.*, *94*, 6581, 1989.

Guckenheimer, J., and P. Holmes, *Nonlinear Oscillations, Dynamical Systems, and Bifurcations of Vector Fields*, Springer-Verlag, New York, 1983.

Haken, H., Cooperative effects in systems far from thermal equilibrium and in nonphysical systems, *Rev. Mod. Phys.*, *47*, 67, 1975.

Haken, H., *Synergetics: An Introduction*, Springer-Verlag, New York, 1983.

Henderson, M. G., G. D. Reeves, and R. D. Belian, Multipoint observations of untriggered substorms, *Eur. Space Agency Spec. Publ., ESA SP-389*, 273, 1996.

Hernandes, J. V., T. Tajima, and W. Horton, Neural net forecasting for geomagnetic activity, *Geophys. Res. Lett.*, *20*, 2707, 1993.

Horton, W., and I. Doxas, A low-dimensional energy conserving state space model for substorm dynamics, *J. Geophys. Res.*, *101*, 27,223, 1996.

Horton, W., and I. Doxas, A low-dimensional dynamical model for the solar wind driven geotail-ionosphere system, *J. Geophys. Res.*, *103*, 4561, 1998.

Horton, W., M. Pekker, and I. Doxas, Magnetic energy storage and the nightside magnetosphere-ionosphere coupling, *Geophys. Res. Lett., 25*, 4083, 1998.

Horton, W., J. P. Smith, R. S. Weigel, C. Crabtree, I. Doxas, B. Goode, and J. Cary, The solar-wind driven magnetosphere-ionosphere as a complex dynamical system, *Phys. Plasmas, 6*, 4178, 1999.

Hurricane, O. A., B. H. Fong, S. C. Cowley, F. V. Coroniti, C. F. Kennel, and R. Pellat, Substorm detonation - the unification of substorm trigger mechanisms, in *Substorms-4: International Conference on Substorms-4, Lake Hamana, Japan, March 9-13, 1998*, edited by S. Kokubun and Y. Kamide, p. 373, Terra Sci., Tokyo, 1998.

Jensen, H. J., *Self-Organized Criticality: Emergent Complex Behavior in Physical and Biological Systems*, Cambridge Univ. Press, New York,1998.

Kamide, Y., et al., Changes in the global electric fields and currents for March 17-19, 1978 from six IMS meridian chains of magnetometers, *Rep. UAG-87*, World Data Cent. A, Boulder, Colo., 1982.

Klimas, A. J., D. N. Baker, D. A. Roberts, D. H. Fairfield,, and J. Büchner, A nonlinear dynamical analogue model of geomagnetic activity, *J. Geophys. Res., 97*, 12,253, 1992.

Klimas, A. J., D. Vassiliadis, D. N. Baker, and D. A. Roberts, The organizaed nonlinear dynamics of the magnetosphere, *J. Geophys. Res., 101*, 13,089, 1996.

Klimas, A. J., D. Vassiliadis, and D. N. Baker, Data-derived analogues of the magnetospheric dynamics, *J. Geophys. Res., 102*, 26,993, 1997.

Landau, L. D., Zur Theorie der Phasenumwandlungen I, *Phys. Z. Sowjetunion, 11*, 26, 1937.

Landau, L. D., and E. M. Lifshitz, *Course of Theoretical Physics*, vol.5, *Statistical Physics*, 266 pp., Addison-Wesley-Longman-Reading, Mass., 1974.

Lembege, B., and R. Pellat, Stability of a thick two-dimensional quasineutral sheet, *Phys. Fluids, 25*, 1995, 1982.

Lewis, Z. V., On the apparent randomness of substorm onset, *Geophys. Res. Lett., 18*, 1627, 1991.

Lui, A. T. Y., Multiscale and intermittent nature of current disruption in the magnetotail, in *Physics of Space Plasmas*, vol.15, edited by T. Chang and J. R. Jasperse, p.233, Mass. Inst. Technol. Cent. for Geo/Cosmo Plasma Phys., Cambridge, 1998.

Lyons, L. R., A new theory for magnetospheric substorms, *J. Geophys. Res., 100*, 19,065, 1995.

Nagel, S. R., Instabilities in a sandpile, *Rev. Mod. Phys., 64*, 321, 1992.

Ohtani, S., T. Higuchi, A. T. Y. Lui, and K. Takahashi, Magnetic fluctuations associated with tail current disruption: Fractal analysis, *J. Geophys. Res., 100*, 19,135, 1995.

Ohtani, S., T. Higuchi, A. T. Y. Lui, and K. Takahashi, AMPTE/CCE-SCATHA simultaneous observations of substorm associated magnetic fluctuations, *J. Geophys. Res., 103*, 4671, 1998.

O'Shea, An exposition of catastrophe theory and its applications to phase transitions, in *Quin's Papers in Pure and Applied Mathemetics*, vol.47, p.1, Queen's Univ., Kingston, Ontario, 1977.

Pellat, R., F. V. Coroniti, and P. L. Pritchett, Does ion tearing exist?, *Geophys. Res., Lett., 18*, 143, 1991.

Preisendorfer, R. W., *Principal Component Analysis in Meteorology and Oceanography*, 425 pp., Elsevier, New York, 1988.

Press, W. H., B.P. Flannery, S. A. Teukolsky, and W. V. Vetterling, *Numerical Recipes: The Art of Scientific Computing*, 2nd ed., Cambridge Univ. Press, New York, 1992.

Pritchard, D., J. E. Borovsky, P. M. Lemons, and C. P. Price, Time dependence of substorm recurrence: An information theoretic analysis, *J. Geophys. Res., 101*, 15,359, 1996.

Pytte, T., R. L. McPherron, E. W. Hones Jr., and H. I. West Jr., Multiple-satellite studies of magnetospheric substorms: Distinction between polar substorms and convection-driven magnetic bays, *J. Geophys. Res., 83*, 663, 1978.

Roberts, D. A., Is there a strange attractor in the magnetosphere?, *J. Geophys. Res., 96*, 16,031, 1991.

Rostoker, G., Triggering of expansion phase intensifications of magnetospheric substorm by northward turning of the interplanetary magnetic field, *J. Geophys. Res., 88*, 6,981, 1983.

Sergeev, V. A., T. I. Pulkkinen, and R. J. Pellinen, Coupled mode scenario for the magnetospheric dynamics, *J. Geophys. Res., 101*, 13,047, 1996a.

Sergeev, V. A., R. J. Pellinen, and T. I. Pulkkinen, Steady magnetospheric convection: A review of recent results, *Space Sci. Rev, 75*, 551, 1996b.

Sharma, A. S., Reconstruction of phase space from time series data by singular spectrum analysis, in *Physics of Space Plasmas*, vol.13,edited by T. Chang and J. R. Jasperse, p.423, Mass. Inst. Technol. Cent. for Theor. Geo/Cosmo Plasma Phys., Cambridge, 1993.

Sharma, A. S., Assessing the magnetosphere's nonlinear behaviour: Its dimension is low, its predictability is high, *Rev. Geophys., 33*, supp., 645, 1995.

Sharma, A. S., D. V. Vassiliadis, and K. Papadopoulos, Reconstruction of low-dimensional magnetospheric dynamics by singular spectrum analysis, *Geophys. Res. Lett., 20*, 335, 1993.

Sitnov, M. I., and A. S. Sharma, Role of transient electrons and microinstabilities in the tearing instability of the geomagnetotail current sheet and the general scenario of the substorm as a catastrophe, in *Substorms-4: International Conference on Substorms-4, Lake Hamana, Japan, March 9-13, 1998*, edited by S. Kokubun and Y. Kamide, p. 539, Terra Sci., Tokyo, 1998.

Sitnov, M. I., H. V. Malova, and A. T. Y. Lui, Quasi-neutral sheet tearing instability induced by electron preferential acceleration from stochasticity, *J. Geophys. Res., 102*, 163, 1997.

Sitnov, M. I., H. V. Malova, and A. S. Sharma, Role of the temperature ratio in the linear stability of the quasi-neutral sheet tearing mode, *Geophys. Res. Lett., 25*, 269, 1998.

Sitnov, M. I., H. V.Malova, and A. S. Sharma, Linear stability of a tearing mode in a quasi-neutral current sheet, *Plasma Phys. Rep., 25*, 227, 1999.

Smith, J.P., and W. Horton, Analysis of the bimodal nature of solar wind-magnetosphere coupling, *J. Geophys. Res., 103*, 14,917, 1998.

Smith, R. A., C. K. Goertz, and W. Grossmann, Thermal catastrophe in the plasma sheet boundary layer, *Geophys. Res. Lett., 13*, 1380, 1986.

Smith, A. J., M. P. Freeman, and G. D. Reeves, Postmidnight VLF chorus events, a substorm signature observed at the ground near L=4, *J. Geophys. Res., 101*, 24,641, 1996.

Stanley, H. E., *Introduction to Phase Transitions and Critical Phenomena*, Oxford Univ. Press, New York, 1971.

Sun, W., W.-Y. Xu, and S.-I. Akasofu, Mathematical separation of directly driven and unloading components in the ionospheric equivalent currents during substorms, *J. Geophys. Res., 103*, 11,695, 1998.

Takalo, J., J. Timonen, and H. Koskinen, Correlation dimension and affinity of *ae* data and bicolored noise, *Geophys. Res. Lett., 20*, 1527, 1993.

Takalo, J., J. Timonen, A. Klimas, J. A. Valdivia, and D. Vassiliadis Nonlinear energy dissipation in a cellular automaton magnetotail field model, *Geophys. Res. Lett.*, *26*, 1813, 1999.

Thom, R., Phase transitions as catastrophes, in *Statistical Mechanics, New Concepts, New Problems, New Applications*, edited by S. A. Rice, K. F. Freed, and J. C. Light, p.93, Univ. of Chicago Press, Chicago, Ill., 1972.

Tsurutani, B., M. Sugiura, T. Iyemori, B. E. Goldstein, W. D. Gonzalez, S.-I. Akasofu, and E. J. Smith, The nonlinear response of AE to the IMF Bs, *Geophys. Res. Lett.*, *17*, 279, 1990.

Vassiliadis, D., A. S. Sharma, T. E. Eastman, and K. Papadopoulos, Low-dimensional chaos in magnetospheric activity from *ae* time seies, *Geophys. Res. Lett.*, *17*, 1841, 1990.

Vassiliadis, D., A. J. Klimas, D. N. Baker, and D. A. Roberts, A description of solar wind-magnetosphere cioupling based on nonlinear filters, *J. Geophys. Res.*, *100*, 3495, 1995.

Vassiliadis, D., A. J. Klimas, D. N. Baker, and D. A. Roberts, The nonlinearity of models of the $vB_{\mathrm{South}} - AL$ coupling, *J. Geophys. Res.*, *101*, 19,779, 1996.

Weigel, R. S., W. Horton, T. Tajima, and T. Detman, Forecasting auroral electrojet activity from solar wind input with neural networks, *Geophys. Res. Lett.*, *26*, 1353, 1999.

Willson, K., The renormalization group and critical phenomena, *Rev. Mod. Phys.*, *55*, 583, 1983.

D. N. Baker, LASP, University of Colorado, Boulder, CO 80302. (baker@lynx.colorado.edu)

A. J. Klimas, Code 692, Laboratory for Extraterrestrial Physics, NASA/Goddard Space Flight Center, Greenbelt, MD 20771. (alex@boken.gsfc.nasa.gov)

K. Papadopoulos, A. S. Sharma and M. I. Sitnov, Department of Astronomy, University of Maryland, College Park, MD 20742. (kp@spp.astro.umd.edu; ssh@astro.umd.edu; sitnov@astro.umd.edu)

J. A. Valdivia, Departamento de Fisica, Facultad de Ciencias, Universidad de Chile, Casilla 653, Santiago, Chile. (alejo@roselott.gsfc.nasa.gov)

D. Vassiliadis, Universities Space Research Association, Code 692, NASA/Goddard Space Flight Center, Greenbelt, MD 20771. (vassi@lepgst.gsfc.nasa.gov)

(Received July 28, 1999; revised December 6, 1999; accepted January 7, 2000.)